Active Control of Optical Signals in the Plasmonic Waveguides

Wen Zhou and Xuguang Huang
Laboratory of Nanophotonic Functional Materials and Devices, School for Information and Optoelectronic Science and Engineering, South China Normal University, Guangzhou, 510006, China.
Email: zhouwscnu@163.com, huangxg@scnu.edu.cn

***Abstract*—In this paper, we review the achievement of active control of optical signals in the nanoscale plasmonic waveguides. They include the ultra-fast all-optical and electro-optical plasmonic switches. The components would be useful in the photonic integrated circuits and the optical communication systems.**

***Index Terms*—SPPs, active plasmonic devices, photonic integrated circuits, signal processing**

I. Introduction

Plasmonic waveguides have attracted much attention because they have potentials to guide light in a region beyond the so-called diffraction limit and are easier to integrate into optical circuits compared with other kinds. They become a strong candidate in realizing highly integrated optical circuits at the subwavelength or nanometer scale. By now, a large number of passive plasmonic waveguide components, such as filters [1-6], splitters, and demultiplexers [7] have been proposed in the previous reports. Those passive components are not enough to construct the optical communication systems including light routing and switching. In this paper, we review the active plasmonic devices demonstrated by our group, including all-optical variable optical attenuators (VOA) [8], all-optical nonlinear switches [9], and ultra-fast electro-optical (EO) switches [10-12], which could meet the above demands.

II. All-Optical Plasmonic VOA/Switches

As shown in Fig. 1(a), the structure of the VOA consists of a MIM waveguide with three teeth cavities filled with a material whose absorption coefficient can be modulated with an external pumping beam. CdSe QD-doped polymethyl methacrylate (PMMA) with refractive index n=2.04+iκ is chosen here. The real part of the refractive index depends on the doping density of CdSe.

The image part κ is the absorption coefficient. In absence of pumping, the QD-doped material is transparent to infrared photons, since their energy is smaller than the QD bandgap. In the presence of pumping, infrared photons are absorbed through an intra-band transition in the QD, the switching are excited by the pump beam. The values of κ of CdSe QD-doped PMMA in the range from 0 to 1 are experimental achievable. Therefore, it is predicted that the transmission characteristics of the structure can be controlled by an external optical beam, and an all-optical functional device will be achieved.

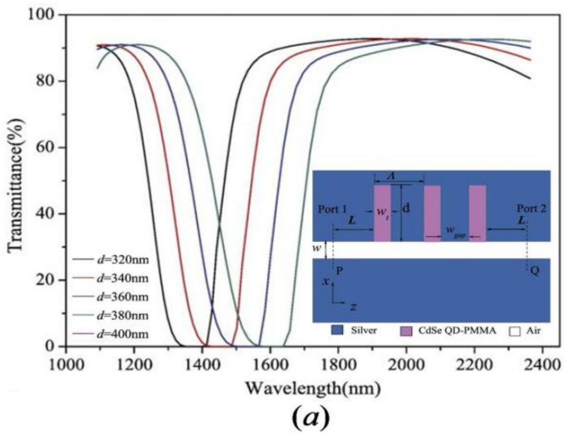

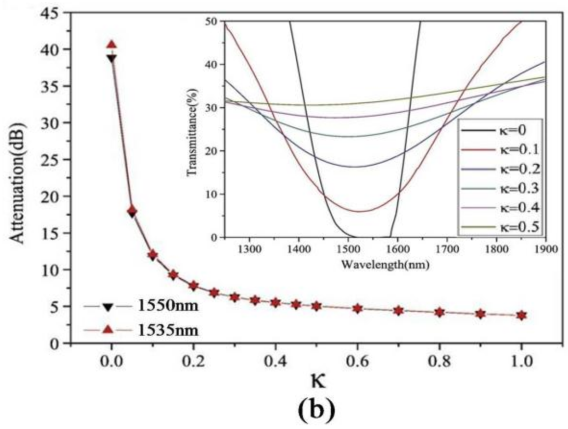

Figure 1. (a) Shift of the forbidden band versus the wavelength for different cavity lengths d. Inset is the schematic of the teeth structure filled with CdSe QD-doped PMMA. (b) The attenuation of the structure versus the imaginary part of the refractive index at 1550nm and 1535nm wavelengths. Inset is the transmission spectra of the structure under optical pumping.

For the sake of comparison, the waveguide width w and the distance L are fixed to be 50nm and 300nm. w_{gap} stands for the width of the gap between any two adjacent cavities. Fig. 1(a) shows simulated transmission spectra of the teeth structure filled with CdSe QD-doped PMMA

Manuscript received July 1, 2013; revised September 28, 2013

doi: 10.12720/ijoee.1.4.304-307

for lengths d=320, 340, 360, 380, and 400nm, with w_t=50nm and Λ=150nm. One can see that increasing the length d shifts the forbidden band to high wavelength, as:

$$\lambda_m = 2(2n_{eff}d + w)/[(2m+1) - \Delta\phi/\pi] \text{ (m=0, 1, 2, ...)}. \quad (1)$$

Inset in Fig. 1(b) shows the transmission spectra of the structure under different optical pumping levels with wt=50nm, d=365nm, Λ=150nm, N=3. One can see that when κ=0 (without pumping), there is a forbidden band of wavelength from 1515nm to 1580nm. The SPP in this wavelength region cannot pass the structure. In presence of optical pumping, the forbidden band disappears, and the transmittance of the structure in the range of 1515-1580nm increases with the increasing of κ. Because the quality factor of the teeth will decrease with the increasing of the absorption of the cavity, the wavelength selection of the teeth cavity will be weakened with the increasing of the absorption coefficient κ. Therefore, the transmittance will increase accordingly.

Fig. 1(b) illustrates the dependence of the attenuation ($-10\log_{10}T$) of the structure on the absorption coefficient κ. The attenuation varies continuously from 39dB to 3.7dB with the increasing of κ at both wavelengths of 1535nm and 1550nm. It reveals that in forbidden band one can control the attenuation of the SPP through the excited-state carrier absorption in CdSe QDs pumped by another light at a different wavelength. Thus the teeth structure filled with CdSe QD-doped PMMA can realize the function of an all-optical broadband VOA.

The structure can also realize all-optical switch function, in which the on/off states correspond to the presence/absence of pumping light. The mechanism of the switch is similar to that of VOA. Without pumping, the teeth operate as a side cavity with a stopband in telecommunication range to reject the light beam passing the structure (off state). In present of a appropriate pumping level, the wavelength selection and the stopband of the teeth cavity are dismissed, and the beam can pass through (on state).

III. ALL-OPTICAL NONLINEAR PLASMONIC SWITCHES

All-optical plasmonic switches based on a novel coupled nanodisk cavity configuration containing nonlinear material are proposed and numerically investigated. The results reveal that the single disk plasmonic structure can operate as an “on–off” switch with the presence/absence of pumping light. We also demonstrate that the proposed T-shaped plasmonic structure with two disk cavities as shown in Fig. 2, can switch signal light from one port to another under an optical pumping light, functioning as a bidirectional switch. The proposed nanodisk cavity plasmonic switches have many advantages such as compact size, requirement of low pumping light intensity, and ultra-fast switching time at a femtosecond scale, which are promising for future integrated plasmonic devices for applications such as communications, signal processing, and sensing.

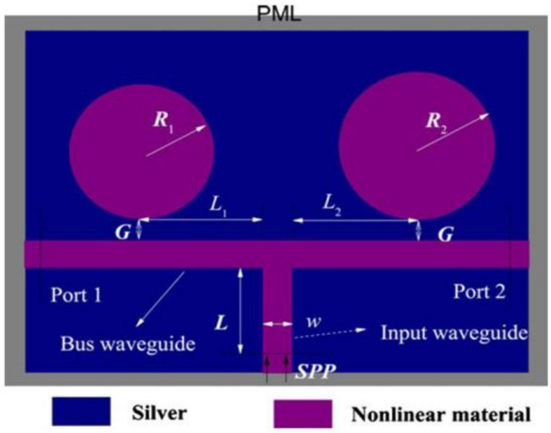

Figure 2. Schematic of a bidirectional all-optical nonlinear plasmonic switch based on two side-coupled nanodisk cavities structures.

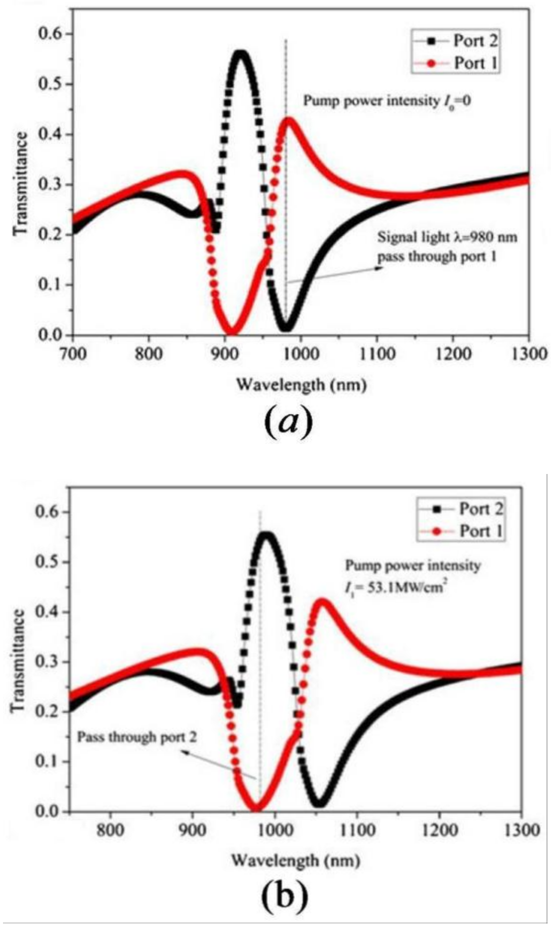

Figure 3. Transmission spectra of two ports of the T-shaped nanodisk structure at different pumping power levels with R_1=140nm, R_2=154nm, and L_1=L_2=350 nm, (a) without the pumping light; (b) with the optical pumping.

As shown in Fig. 3(a), without the pumping light, the light signal at 980nm will be reflected from port 2 by the right-side nanodisk cavity. At the junction of the bus waveguide and the input waveguide, the reflected SPP light signal is divided into two parts: one transmits through port 1 of the bus waveguide and the other passes through the incoming waveguide. The part transmitting through the port 1 will interfere with the incident light passing through the bus waveguide.

It is found that when the pumping intensity is tuned from I_0=0MW/cm^2 to I_1=53.1MW/cm^2, the transmission central wavelength of the notch of the port 1 red-shifts from 910nm to 980nm and the one of the port 2 shifts from 980nm to 1049nm as shown in Fig. 3(b). The resonance wavelength of the left nanodisk cavity changes to 980nm, so the signal light at 980nm will be reflected from the port 1 and passes through the port 2. The transmission of signal light at 980nm jumps from 0.013 to 0.555 for the port 2 when the pumping light (532nm) is increased from 0 to 53.1MW/cm^2, while the transmittance of the port 1 drops from 0.43 to 0.008. And the signal light at 980nm has been directed from the left to the right. Here, we define the transmission contrast ratio of the two ports as $M_t=10\log_{10}(T_{1,2}/T_{2,1})$. With the optical pumping, the light signal is transferred from the left port 1 to the right port 2 and the transmission contrast ratio is 18.4dB.

IV. Electro-Optical Switches

Fig. 4(a) shows the schematic of a 1×2 switch structure composed of two MZI waveguides. The lengths of the two long arms in channels 1 and 2 are equal to $2d_1+L_1$ and $2d_2+L_1$, respectively. V_1 and V_2 are respectively the applied voltages of channels 1 and 2. Fig. 4(b) shows transmission spectra at the two output channels with $d_1=d_2$=190nm, V_1=2.9 V, and V_2=0 V. One can see that channels 1 and 2 can select 655nm and 708nm bands, respectively. Fig. 4(c) shows the transmission spectra at the two output channels for the voltages of V_1=0 V and V_2=2.9 V. Channels 1 and 2 select 708nm and 655nm bands, respectively, at this situation. Therefore, the wavelength at 708nm can be switched from channel 2 to channel 1 when the applied voltages are synchronously tuned from V_1=2.9 V and V_2=0 V into V_1=0 V and V_2=2.9V, while the wavelength at 655nm can be switched from channel 1 to channel 2. It reveals that the waveguide structure is a typical double-wavelength circuit switch. The insertion losses of channels 1 and 2 are respectively -3dB and -1.6dB for 650nm and 708nm wavelength. The extinction ratios of channels 1 and 2 are about 20dB for the wavelength of 655nm and 21dB for 708nm, respectively. Crosstalk is defined as the ratio between the powers of the undesired and desired bands at each output. The crosstalk at channel 1 is around -24dB for the desired wavelength of 655nm, and the crosstalk at channel 2 is -23dB for the wavelength of 708nm.

One of the important parameters of a switch is the switching speed. It is determined by the total summation of the delay time, the material response time, and the rise and fall time of the output optical power. The delay time is defined as the time interval from the beginning of the alteration of the external voltage to the beginning of the alteration of the output optical power, which is the sum of the time for optical beam propagating through the switch and microwave propagating through the electrodes.

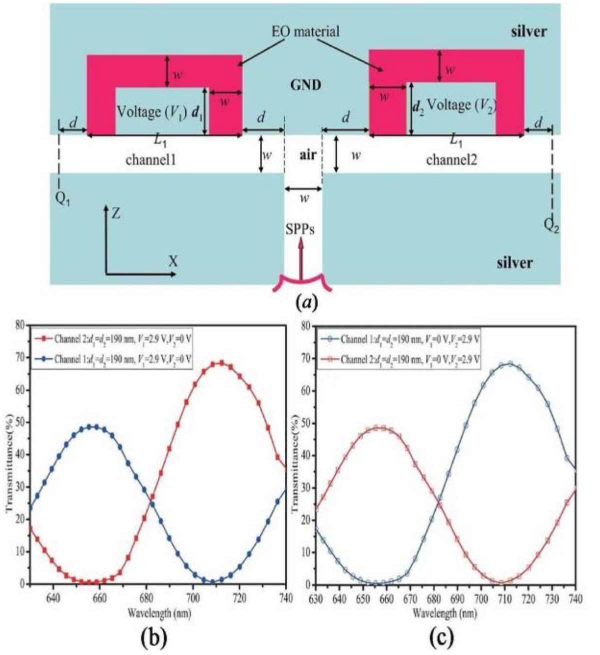

Figure 4. (a) Schematic of a 1×2 electro-optical switch based on double-MZI in T-shaped splitter. (b) Transmission spectra of the 1×2 switch with V_1=2.9 V and V_2=0V. (c) Transmission spectra of the 1×2 switch with V_1=0 V and V_2=2.9 V.

The delay time is on femtosecond order because the lengths of the proposed switch and the electrodes are smaller than 1μm. The bandwidth of the structure is proportional to 1/(RC), here R is loading resistance and C is the capacitance of the structure. In our proposed structure with the width of 50nm, the length smaller than 1μm, and the dielectric constant of about 5, the capacitance is roughly 1fF/μm. Given a typical loading resistance of R=50Ω, the estimated rise time of the proposed switch is～100fs. Consequently, the switching speed of the proposed plasmonic switch is primarily determined by the material response rather than the RC limitations. The proposed structure should be in principle suitable for the operating speed of 20GHz or even higher.

V. Conclusion

According to the above analysis about the all-optical and EO switches, these active plasmonic components have the advantages of low power consumption, nanoscale footprint, ultra-fast speed and broad bandwidth. Our research may provide the possibility to fabricate high-density photonic integration switches with nanoscale.

Acknowledgment

The authors acknowledge the financial support from the National Natural Science Foundation of China (grant no.61077038).

References

[1] X. S. Lin and X. G. Huang, "Tooth-shaped plasmonic waveguide filters with nanometeric sizes," *Opt. Lett*., vol. 33, pp. 2874-2876, December 2008.

[2] J. Tao, X. G. Huang, and S. H. Liu, "Optical characteristics of surface plasmon nanonotch structure," *J. Opt. Soc. Am. B*, vol. 27, pp. 1430-1434, July 2010.

[3] J. Tao, X. G. Huang, X. S. Lin, J. H. Chen, Q. Zhang, and X. P. Jin, "Systematical research on characteristics of double-sided teeth-shaped nanoplasmonic waveguide filters," *J. Opt. Soc. Am. B*, vol. 27, pp. 323-327, September 2010.

[4] J. Tao, X. G. Huang, Q. Zhang, and X. P. Jin, "A narrow-band subwavelength plasmonic waveguide filter with asymmetrical multiple-teeth-shaped structure," *Opt. Express*, vol. 17, pp.13989-13994. August 2009.

[5] Q. Zhang, X. G. Huang, X. S. Lin, J. Tao, and X. P. Jin, "A subwavelength coupler-type MIM optical filter," *Opt. Express*, vol. 17, pp. 7549-7555, April 2009.

[6] X. S. Lin and X. G. Huang, "Numerical modeling of a teeth-shaped nanoplasmonic waveguide filter," *J. Opt. Soc. Am. B*, vol. 26, pp. 1263-1268, July 2009.

[7] J. Tao, X. G. Huang, and J. H. Zhu, "A wavelength demultiplexing structure based on metal-dielectric-metal plasmonic nano-capillary resonators," *Opt. Express*, vol. 18, pp. 11111-11116, May 2010.

[8] J. Tao, X. G. Huang, J. H. Chen, and J. H. Zhu, "All-optical broadband variable optical attenuators and switches in plasmonic teeth waveguides," *Opt. Comm*., vol. 283, pp. 3536-3539, May 2010.

[9] J. Tao, Q. J. Wang, and X. G. Huang, "All-optical plasmonic switches based on coupled nano-disk cavity structures containing nonlinear material," *Plasmonics*, vol. 6, pp. 753-759, December 2011.

[10] J. H. Zhu, X. G. Huang, W. Xu, and L. X. Chen, "Plasmonic optical switches based on mach-zender interferometer," *Phys. Plasmas*, vol. 18, pp. 072112, June 2011.

[11] J. H. Zhu, X. G. Huang, and X. Mei, "Plasmonic electro-optical switches operating at telecom wavelengths," *Plasmonics*, vol. 6, pp. 605-612, May 2011.

[12] X. Mei, X. G. Huang, and J. Tao "A Sub-wavelength electro-optic switch based on plasmonic T-shaped waveguide," *Plasmonics*, vol. 6, pp. 613-618, December 2011.

Wen Zhou was born in Wuhan, China, on September 6, 1989. He received the B.E. degree in physics from the Wuhan Institute of Technology, Hubei, China, in 2011. He has been a postgraduate student in the Laboratory of Nanophotonic Functional Materials and Devices, School of Information and Optoelectronic Science and Engineering, South China Normal University, Guangzhou, China. His major research interests deals with the design and development of novel waveguides and related functional devices, in particular the realization of subwavelength mode confinement and low-loss propagation properties based on photonic crystal waveguides, plasmonic waveguides and their hybrid descendants.

Xuguang Huang received the Ph.D. degree in optics from Sun Yat-sen University, Guangzhou, China, in 1992. He was a Postdoctoral Research Associate with the University of Miami and Rensselaer Polytechnic Institute, Troy, NY, from 1996 to 2000. He was a Senior Product Engineer at two Canada and U.S. fiber-optic technology companies from 2000 to 2003. Since 2004, he has been a Professor in the Laboratory of Nanophotonic Functional Materials and Devices, School of Information and Optoelectronic Science and Engineering, South China Normal University, Guangzhou, China. He has published more than 70 peer-reviewed papers in international academic journals and has two patents. His research interests include integrated photonics, fiber-optic communications, and fiber sensors.